Available online at www.sciencedirect.com
SCIENCE DIRECT®
Composites Science and Technology 64 (2004) 1391–1402
COMPOSITES SCIENCE AND TECHNOLOGY
www.elsevier.com/locate/compscitech

Free vibration analysis of a cantilever composite beam with multiple cracks

Murat Kisa *

Mechanical Engineering Department, Faculty of Engineering, Harran University, Sanliurfa, Turkey

Received 8 July 2003; received in revised form 29 September 2003; accepted 3 November 2003
Available online 19 December 2003

Abstract

This study is an investigation of the effects of cracks on the dynamical characteristics of a cantilever composite beam, made of graphite fibre-reinforced polyamide. The finite element and the component mode synthesis methods are used to model the problem. The cantilever composite beam divided into several components from the crack sections. Stiffness decreases due to cracks are derived from the fracture mechanics theory as the inverse of the compliance matrix calculated with the proper stress intensity factors and strain energy release rate expressions. The effects of the location and depth of the cracks, and the volume fraction and orientation of the fibre on the natural frequencies and mode shapes of the beam with transverse non-propagating open cracks, are explored. The results of the study lead to conclusions that, presented method is adequate for the vibration analysis of cracked cantilever composite beams, and by using the drop in the natural frequencies and the change in the mode shapes, the presence and nature of cracks in a structure can be detected.

Keywords: B. Defects; B. Vibration; C. Finite element analysis; Non-destructive testing; Component mode synthesis

1. Introduction

During operation, all structures are subjected to degenerative effects that may cause initiation of structural defects such as cracks which, as time progresses, lead to the catastrophic failure or breakdown of the structure. Thus, the importance of inspection in the quality assurance of manufactured products is well understood. Several methods, such as non-destructive tests, can be used to monitor the condition of a structure. It is clear that new reliable and inexpensive methods to monitor structural defects such as cracks should be explored. Cracks or other defects in a structural element influence its dynamical behaviour and change its stiffness and damping properties. Consequently, the natural frequencies and mode shapes of the structure contain information about the location and dimensions of the damage. Vibration analysis, which can be used to detect structural defects such as cracks, of any structure offers an effective, inexpensive and fast means of non-destructive testing. What types of changes occur in the vibration characteristics, how these changes can be detected and how the condition of the structure is interpreted has been the topic of several research studies in the past [1–7] and reviewed by many researchers such as Wauer [8] and Dimarogonas [9].

Over the past decade, several techniques have been explored for detecting and monitoring of the defects in the composite materials. Adams et al. [10] showed that any defect in fibre-reinforced plastics could be detected by reduction in natural frequencies and increase in damping. Nikpour and Dimarogonas [11] studied the variation of the mixed term in the energy release rate for various angles of inclination of the material axes of symmetry and they derived the local compliance matrix of a prismatic beam with a central crack. Nikpour [12] studied the buckling of cracked composite columns and showed that the instability increases with the column slenderness and the crack depth. Oral [13] developed a shear flexible finite element for non-uniform laminated composite beams. He tested the performance of the element with isotropic and composite materials, constant and variable cross-sections, and straight and curved

* Tel.: +90-533-4524865; fax: +90-414-3440031.
E-mail address: m.kisa@harran.edu.tr (M. Kisa).

0266-3538/$ - see front matter © 2003 Elsevier Ltd. All rights reserved.
doi:10.1016/j.compscitech.2003.11.002

geometries. Krawczuk [14] developed a new finite element for the static and dynamic analysis of cracked composite beams. He assumed that the crack changes only the stiffness of the element whereas the mass of the element is unchanged. Krawczuk and Ostachowicz [15] investigated the eigenfrequencies of a cracked cantilever composite beam. They presented two models of the beam. In the first model, the crack was modelled by a massless spring and in the second model the cracked part of the beam replaced by a cracked element. Krawczuk et al. [16] proposed an algorithm to find the characteristic matrices of a composite beam with a single transverse fatigue crack. In the literature, exception of a few papers [17–21], where the vibration analysis of beams with two or multiple cracks was explored, there is a small number of research works addressing particularly to the problem of free vibration of composite beams having multiple open-edge cracks. Recently, Song et al. [22] investigated the dynamics of anisotropic composite cantilevers. They presented an exact solution methodology utilising Laplace transform technique to study the bending free vibration of cantilever composite beams with multiple open cracks.

The full eigensolution of a structure containing substructures each having large numbers of degrees of freedom can be cumbersome and costly in computing time. A method proposed by Hurty [23] enabled the problem to be broken up into separate elements and thus considerably reduced its complexity. His method consisted of considering the structure in terms of substructures and was called as 'substructuring'. Essentially, the method required the derivation of the dynamic equations for each component and these equations were then connected mathematically by matrices which represent the physical displacements of interface connection points on each component. In this way, one large eigenproblem is replaced by several smaller ones. In many respects, the original rationale for such substructuring techniques has been rendered obsolete by the widespread availability of high performance computers. However, there are applications where alternative justifications are valid, for example where the results of independent analysis of individual structural modules are to be used to predict the dynamics of an assembled structure. In the present context, the author wishes to examine the response prediction of an assembled structure under a variety of assumptions concerning nonlinearity at the interface of substructures which are otherwise linear.

2. Mathematical model

The model chosen is a cantilever composite beam of uniform cross-section A, having multiple open-edge transverse cracks of various depths a_i at variable positions L_i $(i = 1, \ldots, n)$. The width, length and height of the beam are B, L and H, respectively, Fig. 1. The angle between the fibres and the axis of the beam is α. The

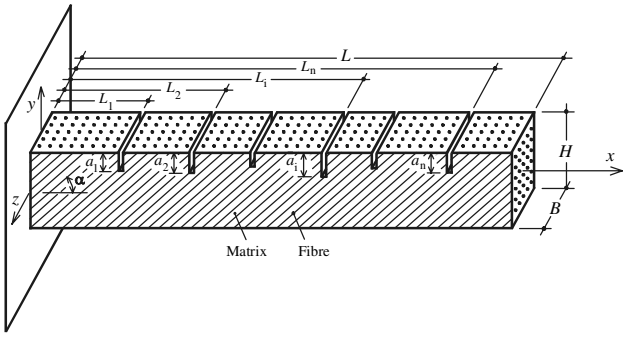

Fig. 1. Geometry of the cantilever composite beam with multiple cracks.

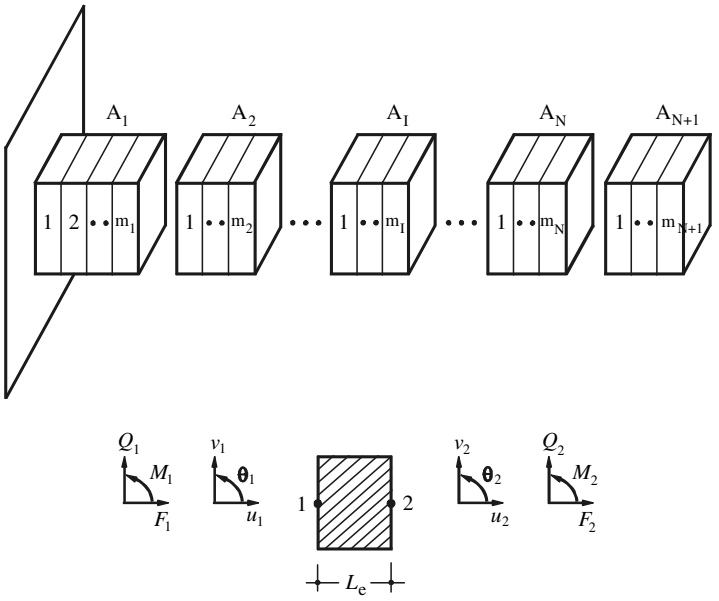

Fig. 2. Components of the composite beam and dividing them into the finite number of elements.

cantilever beam is partitioned into several components from the crack sections enabling a substructure approach, Fig. 2. By separating the whole beam into parts, global non-linear system can be separated into linear subsystems joined by local stiffness discontinuities. In the current study, each component is also divided into finite elements with two nodes and three degrees of freedom at each node as shown in Fig. 2.

2.1. Stiffness and mass matrices for composite beam element

The stiffness and mass matrices are developed from the procedure given by Krawczuk [15] and modified to three degrees of freedom for each node, $\delta = \{u, v, \theta\}$. In Fig. 2, a general finite element, the applied system forces $F = \{F_1, Q_1, M_1, F_2, Q_2, M_2\}$ and the corresponding displacements $\delta = \{u_1, v_1, \theta_1, u_2, v_2, \theta_2\}$ are shown. The stiffness matrix for a two-noded composite beam element with three degrees of freedom $\delta = \{u, v, \theta\}$ at each node, for the case of bending in the xy plane, are given as follows [15]:

$$K_{\mathrm{el}} = [k_{ij}]_{(6\times 6)}, \tag{1}$$

where k_{ij} $(i, j = 1, \ldots, 6)$ are given as

$$\begin{aligned}
k_{11} &= k_{55} = 7BH\bar{S}_{33}/3L_{\mathrm{e}},\\
k_{12} &= k_{21} = -k_{56} = -k_{65} = BH\bar{S}_{33}/2,\\
k_{13} &= k_{31} = k_{35} = k_{53} = -8BH\bar{S}_{33}/3L_{\mathrm{e}},\\
k_{14} &= k_{41} = k_{36} = k_{63} = -k_{23} = -k_{32}\\
&= -k_{45} = -k_{54} = 2BH\bar{S}_{33}/3,\\
k_{15} &= k_{51} = BH\bar{S}_{33}/3L_{\mathrm{e}},\\
k_{16} &= k_{61} = -k_{25} = -k_{52} = -BH\bar{S}_{33}/6,\\
k_{22} &= k_{66} = BH(7H^2\bar{S}_{11}/36L_{\mathrm{e}} + L_{\mathrm{e}}\bar{S}_{33}/9),\\
k_{24} &= k_{42} = k_{46} = k_{64} = BH(-2H^2\bar{S}_{11}/9L_{\mathrm{e}} + L_{\mathrm{e}}\bar{S}_{33}/9),\\
k_{26} &= k_{62} = BH(H^2\bar{S}_{11}/36L_{\mathrm{e}} - L_{\mathrm{e}}\bar{S}_{33}/18),\\
k_{33} &= 16BH\bar{S}_{33}/3L_{\mathrm{e}},\\
k_{44} &= BH(4H^2\bar{S}_{11}/9L_{\mathrm{e}} + 4L_{\mathrm{e}}\bar{S}_{33}/9),\\
k_{34} &= k_{43} = 0,
\end{aligned} \tag{2}$$

where B, H and L_{e} are the dimensions of the composite beam element. $\bar{S}_{11}$ and $\bar{S}_{33}$ are the stress–strain constants and given as [24]

$$S_{11} = \bar{S}_{11}m^4 + 2(\bar{S}_{12} + 2\bar{S}_{33})m^2n^2 + \bar{S}_{22}n^4, \tag{3}$$

$$S_{33} = (\bar{S}_{11} - 2\bar{S}_{12} + \bar{S}_{22} - 2\bar{S}_{33})m^2n^2 + \bar{S}_{33}(m^4 + n^4), \tag{4}$$

where $m = \cos\alpha$, $n = \sin\alpha$ and $\bar{S}_{ij}$ terms are determined from the relations [24]

$$\begin{aligned}
&\bar{S}_{11} = \frac{E_{11}}{(1 - v_{12}^2E_{22}/E_{11})}, \quad \bar{S}_{22} = S_{11}E_{22}/E_{11},\\
&\bar{S}_{12} = v_{12}S_{22}, \quad \bar{S}_{33} = G_{12},
\end{aligned} \tag{5}$$

where E_{11}, E_{22}, G_{12} and v_{12} are the mechanical properties of the composite and can be determined as shown in Appendix A.

The mass matrix of the composite beam element can be given as [15]

$$M_{\mathrm{el}} = [m_{ij}]_{(6\times 6)}, \tag{6}$$

where m_{ij} $(i, j = 1, \ldots, 6)$ are

$$\begin{aligned}
m_{11} &= m_{55} = 2\rho BHL_{\mathrm{e}}/15,\\
m_{12} &= m_{21} = -m_{56} = -m_{65} = \rho BHL_{\mathrm{e}}^2/180,\\
m_{13} &= m_{31} = m_{35} = m_{53} = \rho BHL_{\mathrm{e}}/15,\\
m_{14} &= m_{41} = -m_{45} = -m_{54} = -\rho BHL_{\mathrm{e}}^2/90,\\
m_{36} &= m_{63} = m_{23} = m_{32} = m_{34} = m_{43} = 0,\\
m_{15} &= m_{51} = -\rho BHL_{\mathrm{e}}/30,\\
m_{16} &= m_{61} = -m_{25} = -m_{52} = \rho BHL_{\mathrm{e}}^2/180,\\
m_{22} &= m_{66} = \rho BHL_{\mathrm{e}}(L_{\mathrm{e}}^2/1890 - H^2/360),\\
m_{24} &= m_{42} = m_{46} = m_{64}\\
&= \rho BHL_{\mathrm{e}}(-L_{\mathrm{e}}^2/945 + H^2/180),\\
m_{26} &= m_{62} = \rho BHL_{\mathrm{e}}(L_{\mathrm{e}}^2/1890 - H^2/360),\\
m_{33} &= 8\rho BHL_{\mathrm{e}}/15,\\
m_{44} &= \rho BHL_{\mathrm{e}}(2L_{\mathrm{e}}^2/945 + 2H^2/45),
\end{aligned} \tag{7}$$

where ρ is the mass density of the element.

2.2. The stiffness matrix for the crack

According to the St. Venant's principle, the stress field is influenced only in the region near to the crack. The additional strain energy due to crack leads to flexibility coefficients expressed by stress intensity factors derived by means of Castigliano's theorem in the linear elastic range. In this study, the bending-stretching effect due to mid-plane asymmetry induced by the cracks is neglected. The compliance coefficients C_{ij} induced by crack are derived from the strain energy release rate, J, developed in Griffith–Irwin theory [25]. J can be given as

$$J = \frac{\partial U(P_i, A)}{\partial A}, \tag{8}$$

where A is the area of the crack section, P_i are the corresponding loads, U is the strain energy of the beam due to crack and can be expressed as [11]

$$U = \int_A \left(D_1 \sum_{i=1}^{i=N} K_{\mathrm{I}i}^2 + D_{12} \sum_{i=1}^{i=N} K_{\mathrm{I}i} \sum_{j=1}^{j=N} K_{\mathrm{II}j} + D_2 \sum_{i=1}^{i=N} K_{\mathrm{II}i}^2 \right) \mathrm{d}A, \tag{9}$$

where K_{I} and K_{II} are the stress intensity factors for fracture modes of I and II. D_1, D_{12} and D_2 are the coefficients depending on the materials parameters [11]

$$D_1 = -0.5\bar{b}_{22}\,\mathrm{Im}\left(\frac{s_1 + s_2}{s_1 s_2}\right), \tag{10}$$

$$D_{12} = \bar{b}_{11}\,\mathrm{Im}(s_1 s_2), \tag{11}$$

$$D_2 = 0.5\bar{b}_{11}\,\mathrm{Im}(s_1 + s_2). \tag{12}$$

The coefficients s_1, s_2 and $\bar{b}_{ij}$ are given in Appendix A. The mode I and II stress intensity factors, K_I and K_II, for a composite beam with a crack are expressed as [26]

$$K_{ji} = \sigma_i\sqrt{\pi a}\,Y_j(\xi)F_{ji}(a/H), \tag{13}$$

where σ_i is the stress for the corresponding fracture mode, $F_{ji}(a/H)$ is the correction factor for the finite specimen size, $Y_j(\xi)$ is the correction factor for the anisotropic material [11], a is the crack depth and H is the element height. Castigliano's theorem [27] implies that the additional displacement due to crack, according to the direction of the P_i, is

$$u_i = \frac{\partial U(P_i, A)}{\partial P_i}. \tag{14}$$

Substituting the strain energy release rate J into Eq. (14), the relation between displacement and strain energy release rate J can be written as follows:

$$u_i = \frac{\partial}{\partial P_i}\int_A J(P_i, A)\,\mathrm{d}A. \tag{15}$$

The flexibility coefficients, which are the functions of the crack shape and the stress intensity factors, can be introduced as follows [25]:

$$c_{ij} = \frac{\partial u_i}{\partial P_j} = \frac{\partial^2}{\partial P_i \partial P_j}\int_A J(P_i, A)\,\mathrm{d}A = \frac{\partial^2 U}{\partial P_i \partial P_j}. \tag{16}$$

The compliance coefficients matrix, after being derived from above equation, can be given according to the displacement vector $\delta = \{u, v, \theta\}$ as

$$C = [c_{ij}]_{(3\times 3)}, \tag{17}$$

where c_{ij} $(i, j = 1, 2, 3)$ are derived by using Eqs. (8)–(16).

The inverse of the compliance coefficients matrix, C^{-1}, is the stiffness matrix due to crack. Considering the cracked node as a cracked element of zero length and zero mass [5], the crack stiffness matrix can be represented by equivalent compliance coefficients. Finally, resulting stiffness matrix for the crack can be given as

$$K_\mathrm{c} = \begin{bmatrix} [C]^{-1} & -[C]^{-1} \\ -[C]^{-1} & [C]^{-1} \end{bmatrix}_{(6\times 6)}. \tag{18}$$

3. Component mode analysis

The equation of motion of a mid-plane symmetrical composite beam is [24]

$$IS_{11}\partial^4 y(x,t)/\partial x^4 + \rho A\partial^2 y(x,t)/\partial t^2 = f(t), \tag{19}$$

where I, ρ, A and $y(x,t)$ are the geometrical moment of inertia of the beam cross-section, material density, cross-sectional area of the beam and transverse deflection of the beam, respectively. Now, consider the component A_1, Fig. 2, for undamped vibration analysis, Eq. (19), in matrix notation, can be given as

$$M_{\mathrm{A}_1}\ddot{q}_{\mathrm{A}_1} + K_{\mathrm{A}_1} q_{\mathrm{A}_1} = f_{\mathrm{A}_1}(t), \tag{20}$$

where M_{A_1} and K_{A_1} are the mass and stiffness matrices of the component A_1, respectively, q_{A_1} and $f_{\mathrm{A}_1}(t)$ are the generalised displacement and external force vectors, respectively. Assuming that

$$\begin{aligned} \{q_{\mathrm{A}_1}\} &= \{\phi_{\mathrm{A}_1}\}\sin(\omega_{\mathrm{A}_1} t + \beta), \\ \{\ddot{q}_{\mathrm{A}_1}\} &= -\omega^2_{\mathrm{A}_1}\{\phi_{\mathrm{A}_1}\}\sin(\omega_{\mathrm{A}_1} t + \beta) \end{aligned} \tag{21}$$

and substituting them into Eq. (20), one ends up with the standard free vibration equation for the component A_1 as,

$$\omega^2_{\mathrm{A}_1} M_{\mathrm{A}_1}\phi_{\mathrm{A}_1} = K_{\mathrm{A}_1}\phi_{\mathrm{A}_1}, \tag{22}$$

which gives eigenvalues $\omega^2_{\mathrm{A}_1 1}, \ldots, \omega^2_{\mathrm{A}_1 n}$ and modal matrix ϕ_{A_1} for the component A_1. Making the transformation

$$q_{\mathrm{A}_1} = \phi_{\mathrm{A}_1} p_{\mathrm{A}_1}, \tag{23}$$

where p_{A_1} is the principal coordinate vector. By premultiplying $\phi^\mathrm{T}_{\mathrm{A}_1}$ and substituting Eq. (23), Eq. (20) becomes

$$(\phi^\mathrm{T}_{\mathrm{A}_1} M_{\mathrm{A}_1}\phi_{\mathrm{A}_1})\ddot{p}_{\mathrm{A}_1} + (\phi^\mathrm{T}_{\mathrm{A}_1} K_{\mathrm{A}_1}\phi_{\mathrm{A}_1})p_{\mathrm{A}_1} = \phi^\mathrm{T}_{\mathrm{A}_1} f_{\mathrm{A}_1}(t), \tag{24}$$

where

$$\begin{aligned} \phi^\mathrm{T}_{\mathrm{A}_1} M_{\mathrm{A}_1}\phi_{\mathrm{A}_1} &= [m_m], \\ \phi^\mathrm{T}_{\mathrm{A}_1} K_{\mathrm{A}_1}\phi_{\mathrm{A}_1} &= [k_m], \end{aligned} \tag{25}$$

where $[m_m]$ and $[k_m]$ are modal mass and stiffness matrices, respectively. Mass normalising the modal matrix by

$$\psi_{ij} = \frac{\phi_{ij}}{\sqrt{m_{jj}}}, \tag{26}$$

where ψ_{ij} is mass normalised mode vector. By using the transformation

$$q_{\mathrm{A}_1} = \psi_{\mathrm{A}_1} s_{\mathrm{A}_1} \tag{27}$$

by premultiplying $\psi^\mathrm{T}_{\mathrm{A}_1}$ and substituting Eq. (27), Eq. (20) becomes

$$I\ddot{s}_{\mathrm{A}_1} + \omega^2_{\mathrm{A}_1} s_{\mathrm{A}_1} = \psi^\mathrm{T}_{\mathrm{A}_1} f_{\mathrm{A}_1}(t), \tag{28}$$

where $\omega^2_{\mathrm{A}_1}$ is a diagonal matrix comprising the eigenvalues of A_1.

3.1. Coupling of the components

Consider components, $\mathrm{A}_1, \mathrm{A}_2, \ldots, \mathrm{A}_N$, joined together by means of springs capable of carrying axial, shearing and bending effects, Fig. 3. The kinetic and strain energy of the components, in terms of principal modal coordinates, can be given as

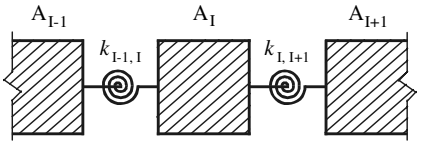

Fig. 3. Composite beam components connected by springs.

$$T = \frac{1}{2}\dot{s}^{\mathrm{T}} M \dot{s}, \qquad U = \frac{1}{2} s^{\mathrm{T}} K s, \tag{29}$$

where T and U are kinetic and strain energy, respectively. M and K in Eq. (29) are

$$M = \begin{bmatrix} I & 0 & \cdots & 0 \\ 0 & I & \cdots & 0 \\ \cdots & \cdots & \cdots & \cdots \\ 0 & 0 & \cdots & I \end{bmatrix}, \qquad K = \begin{bmatrix} \omega_{\mathrm{A}_1}^2 & 0 & \cdots & 0 \\ 0 & \omega_{\mathrm{A}_2}^2 & \cdots & 0 \\ \cdots & \cdots & \cdots & \cdots \\ 0 & 0 & \cdots & \omega_{\mathrm{A}_N}^2 \end{bmatrix}. \tag{30}$$

The strain energy of the connectors, in terms of principal modal coordinates, is

$$U_{\mathrm{C}} = \frac{1}{2} s^{\mathrm{T}} \psi^{\mathrm{T}} K_{\mathrm{C}} \psi s, \tag{31}$$

where K_{C} is the stiffness matrix of the cracked nodal element and can be calculated by using Eq. (18). ψ in Eq. (31) can be written as

$$\psi = \begin{bmatrix} \psi_{\mathrm{A}_1} & 0 & \cdots & 0 \\ 0 & \psi_{\mathrm{A}_2} & \cdots & 0 \\ \cdots & \cdots & \cdots & \cdots \\ 0 & 0 & \cdots & \psi_{\mathrm{A}_N} \end{bmatrix}. \tag{32}$$

The total strain energy of the system is, therefore,

$$U_{\mathrm{T}} = \frac{1}{2} s^{\mathrm{T}} (K + \psi^{\mathrm{T}} K_{\mathrm{C}} \psi) s, \tag{33}$$

where K has been given by Eq. (30). The equation of motion of the complete structure is

$$\ddot{s} + (K + \psi^{\mathrm{T}} K_{\mathrm{C}} \psi) s = \psi^{\mathrm{T}} f(t), \tag{34}$$

where ψ has been given by Eq. (32), $f(t)$ is the global force vector for the system. From Eq. (34), the eigenvalues and mode shapes of the cracked system can be determined. After solving these equations, the displacements for each component are calculated by using Eq. (27).

4. Results and discussion

4.1. Validation of the current approach

In order to check the accuracy of the present method, the case considered in [16] is adopted here. The beam assumed to be made of unidirectional graphite fibre-reinforced polyamide. The geometrical characteristics and material properties of the beam were chosen as the same of those used in [16]. The material properties of the graphite fibre-reinforced polyamide composite, in terms of fibres and matrix, identified by the indices f and m, respectively, are

Modulus of elasticity	$E_{\mathrm{m}} = 2.756$ GPa, $E_{\mathrm{f}} = 275.6$ GPa
Modulus of rigidity	$G_{\mathrm{m}} = 1.036$ GPa, $G_{\mathrm{f}} = 114.8$ GPa
Poisson's ratio	$v_{\mathrm{m}} = 0.33$, $v_{\mathrm{f}} = 0.2$
Mass density	$\rho_{\mathrm{m}} = 1600$ kg/m^3, $\rho_{\mathrm{f}} = 1900$ kg/m^3

The geometrical characteristics, the length (L), height (H) and width (B) of the composite beam, as consistent with [16], were chosen as 0.6 m, 0.025 m and 0.05 m, respectively.

Firstly, the presented method has been applied for the free vibration analysis of a non-cracked composite cantilever beam. The three lowest eigenfrequencies for various values of the angle of the fibre (α) and the volume fraction of fibres (V) are determined. As shown in Fig. 4, the results found by using a four elements model are compared with the analytical and numerical solutions found in the literature [16,24]. The non-dimensional natural frequencies are normalised according to the following relation [16]:

$$\varpi_i = L\sqrt{\omega_i H / \sqrt{\bar{S}_{11}/12\rho}}, \tag{35}$$

where L and H show the length and height of the beam, respectively. ω_i is the ith dimensional natural frequency. As can be seen from the figures, an excellent agreement has been found between the results.

Secondly, the natural frequencies and mode shapes of the cantilever composite beam having single open-edge crack are analysed. The calculations have been carried out for various volume fractions of the fibres (V), the fibre angles (α) and the crack ratios (a/H). The natural frequencies of the cracked cantilever composite beam are lower than those of the corresponding intact beam, as expected. In Fig. 5, the changes in the first natural frequency of the cracked beam are given as a function of the different crack ratios (a/H) and the fibre orientations (α) for several volume fractions (V). First non-dimensional natural frequencies are normalised according to the following equation:

$$\omega = \frac{\omega(\alpha)}{\omega_{\mathrm{nc}}(\alpha)}, \tag{36}$$

where $\omega(\alpha)$ and $\omega_{\mathrm{nc}}(\alpha)$ denote the natural frequency of the cracked and non-cracked cantilever composite beam as a function of the angle of the fibre (α), respectively. As seen in Fig. 5, when the crack is perpendicular to the fibre direction, the decrease in the first natural frequency

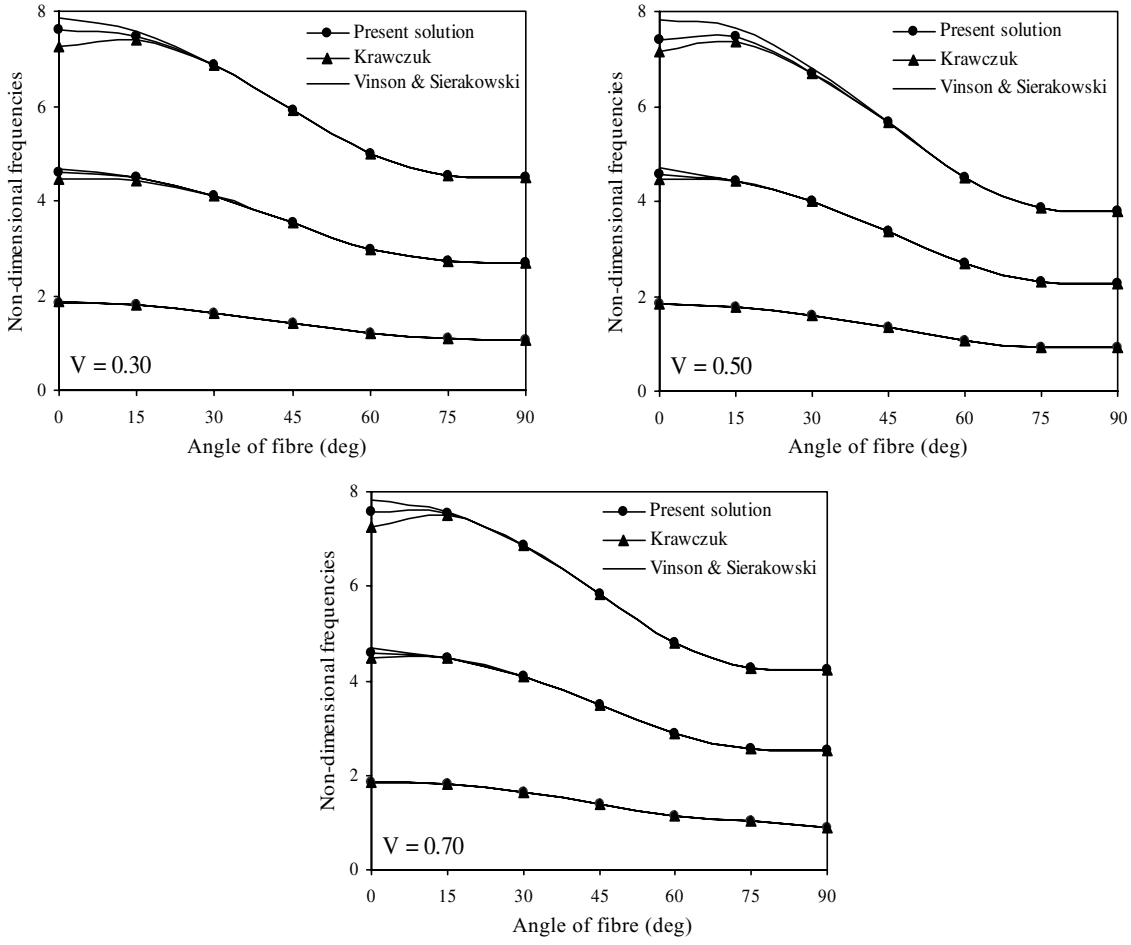

Fig. 4. Non-dimensional natural frequencies of the intact composite beam as a function of the fibre angle α.

is highest. As the angle of the fibre increases, the changes in the first frequency reduce. For the value of the angle of fibre is greater than 45° these changes are very low and thus, the fundamental frequency of the cantilever composite beam with cracks does not differ too much from that of the corresponding non-cracked beam. Fig. 5 shows that the reduction in the first natural frequency is higher for the volume fraction of the fibres is between 0.3 and 0.5.

In Fig. 6, the variation of the first natural frequencies of the cracked cantilever composite beam is presented as a function of relative crack positions (L_1/L) and depths (a/H). In the analysis, the volume and angle of fibre were assumed to be 0.1 and 0°, respectively. Non-dimensional natural frequencies are normalised according to Eq. (36). Due to the bending moment along the beam, which is concentrated at the fixed end, a crack near the free end will have a smaller effect on the fundamental frequency than a crack closer to the fixed end, and as seen from Fig. 6, it can be concluded that the frequencies are almost unchanged when the crack is located away from the fixed end. These conclusions are in perfect agreement to those outlined by Krawczuk and Ostachowicz [16].

4.2. Vibration of composite beam with multiple cracks

After verification of the present method, the approach is applied to a composite beam with multiple cracks as shown in Fig. 1. The numerical illustrations were carried out for a composite cantilever beam having the same geometrical characteristics and material properties as the ones supplied in [22]. The material properties of the composite beam were the same as those used in the previous case. The geometrical beam characteristics, consistent with [22], were $L = 1$ m, $H = 0.025$ m, $B = 0.025$ m.

In Fig. 7, the variation of the first three lowest natural frequencies of the composite beam with multiple cracks is shown as a function of fibre orientation (α) for the different crack locations (L_i/L). In this figure, three cases, labelled as E, F and G, were considered. In the model, the number of the cracks assumed to be three. The crack locations (L_1/L, L_2/L, L_3/L) for the cases E, F and G, were chosen as, $(0.05, 0.15, 0.25)$, $(0.45, 0.55, 0.65)$, $(0.75, 0.85, 0.95)$, respectively. For numerical calculations, the volume of the fibre (V) and the crack ratio (a/H) were assumed to be 0.5 and 0.2, respectively. The non-dimensional natural frequencies, for the present and subsequent cases, are normalised according to Eq. (36).

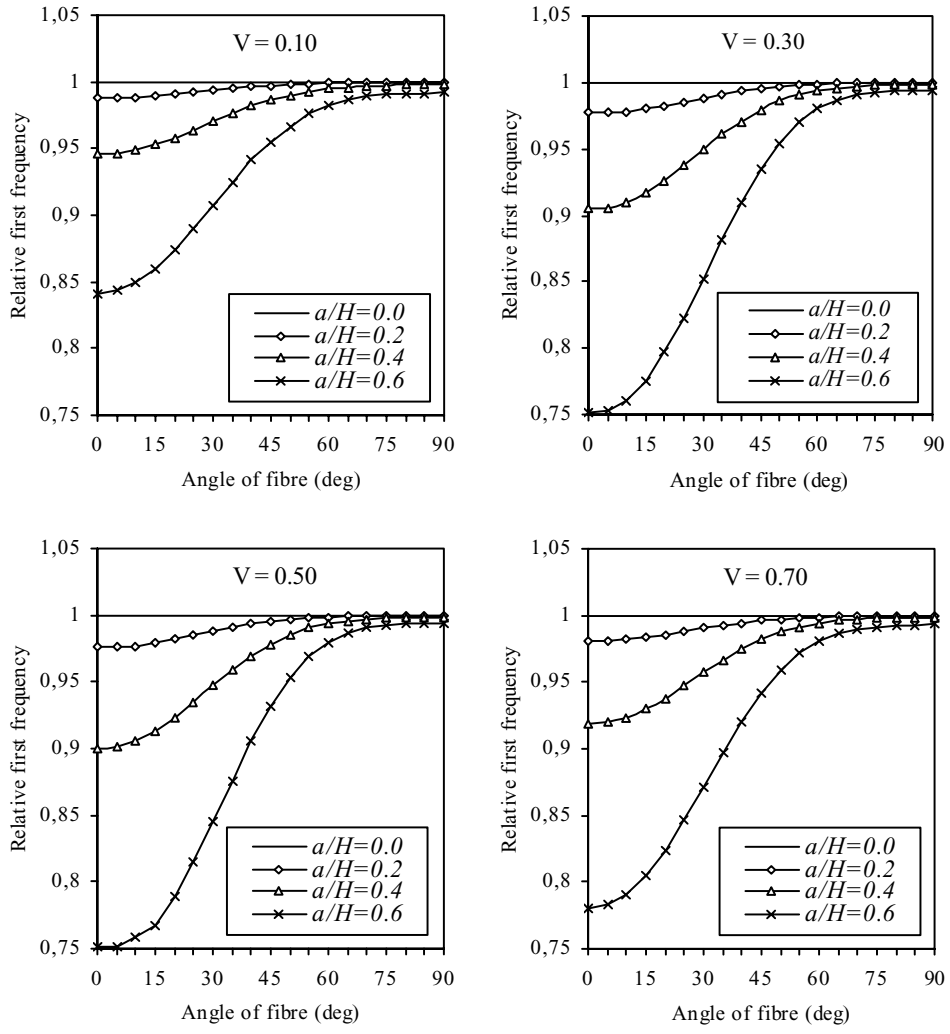

Fig. 5. Changes in the first natural frequency of the cracked composite beam as a function of the angle of fibre for various crack ratios.

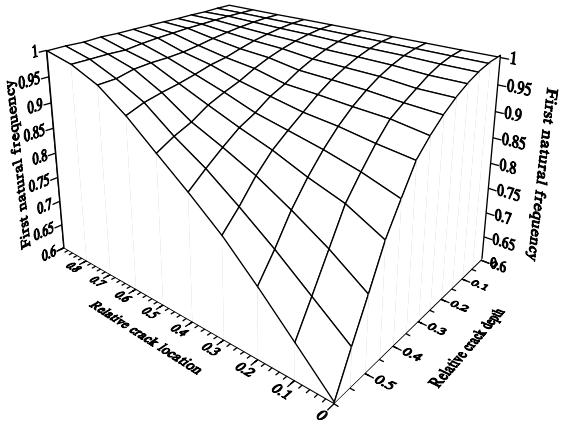

Fig. 6. Changes in the first natural frequency for various relative crack depth and location.

It can be clearly seen from the Fig. 7 that, when the cracks are placed near the fixed end the decreases in the first natural frequency are highest, whereas, when the cracks are located near the free end, the first natural frequencies are almost unaffected. This observation goes to the conclusion that, the first, second and third natural frequencies are most affected when the cracks located at the near of the fixed end, the middle of the beam and the free end, respectively, Fig. 7. This conclusion is clearly seen from Fig. 8, which illustrates the first three natural bending mode shapes of the cracked composite beam.

Fig. 9 shows the first three natural frequencies as a function of the fibre orientation (α) for different crack ratios (a/H). In the model, the composite beam has four cracks which were located as $L_1/L = 0.05$, $L_2/L = 0.35$, $L_3/L = 0.65$, $L_4/L = 0.95$, and the volume of fibre (V) was 0.5. It is noticeable that decreases in the natural frequencies become more intensive with the growth of the crack depth. The most difference in frequency occurs when the angle of the fibre (α) is 0°. When the value of the angle of fibre is greater than 45°, the effects of the cracks on the frequencies decrease. This can be

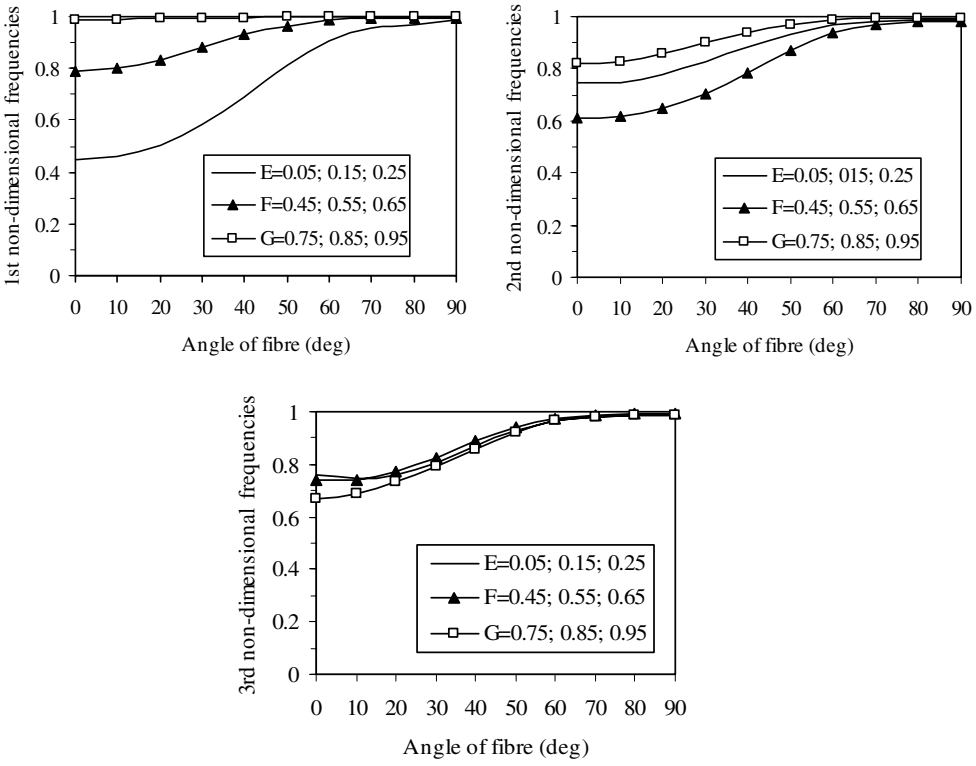

Fig. 7. Variation of the first three non-dimensional natural frequencies as a function of fibre orientation for the case of three cracks located differently, as indicated $a/H = 0.2$ and $V = 0.5$.

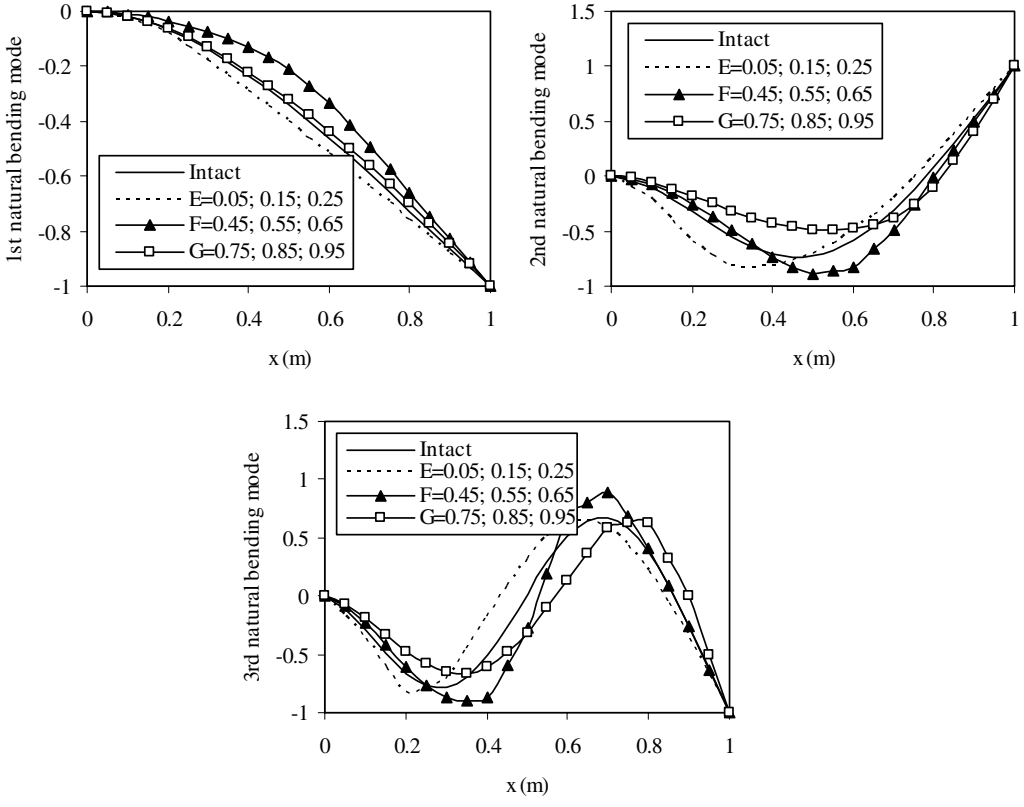

Fig. 8. Normalised first three mode shapes that correspond to the cases in Fig. 7.

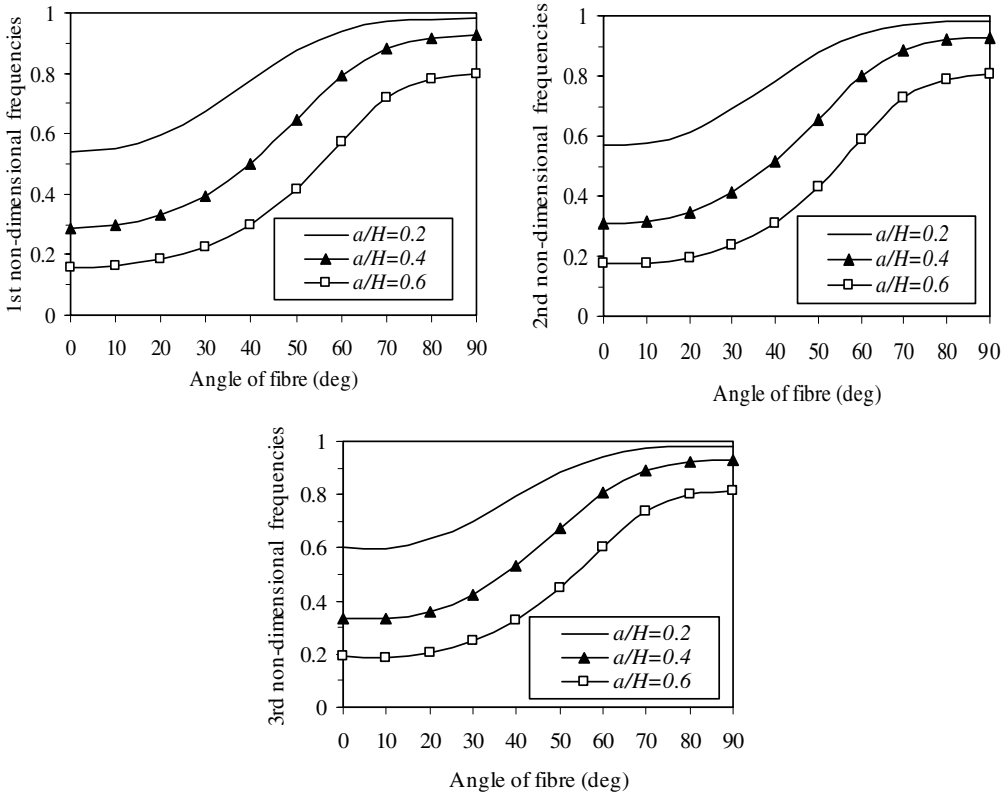

Fig. 9. First three non-dimensional natural frequencies as a function of fibre orientation for different crack ratios $a/H = 0.2, 0.4, 0.6$, volume of the fibre V is 0.5.

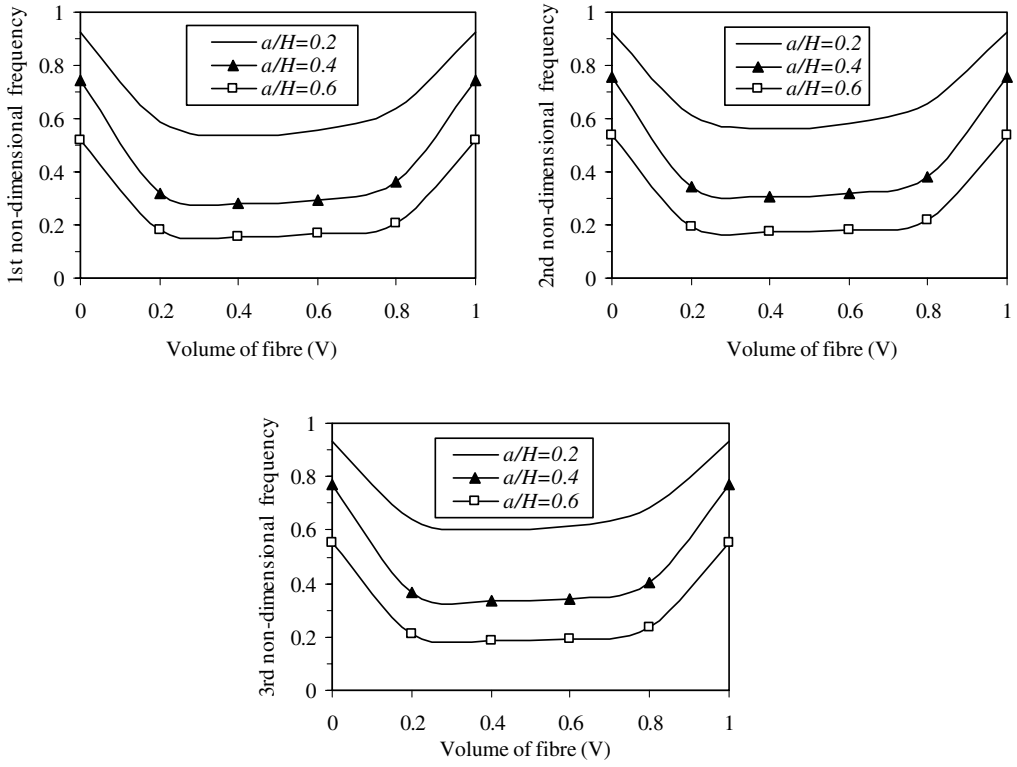

Fig. 10. First three non-dimensional natural frequencies as a function of the fibre volume fraction for different crack ratios $a/H = 0.2, 0.4, 0.6$, angle of the fibre α is 0°.

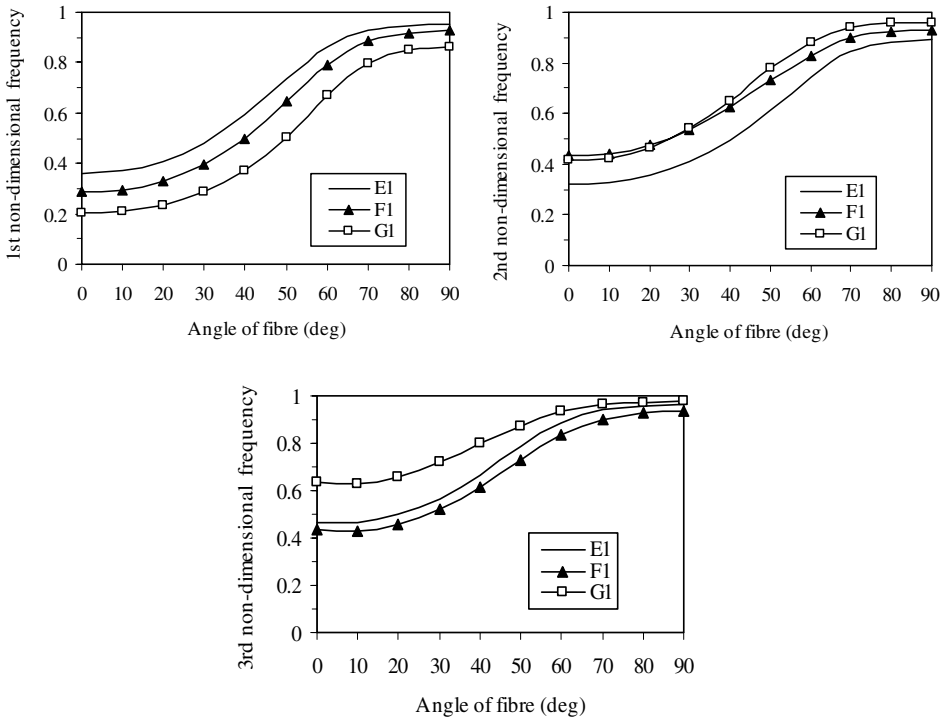

Fig. 11. Variation of the first three non-dimensional natural frequencies as a function of fibre orientation for the case of three cracks featuring various depths. For the cases E_1, F_1 and G_1, the crack locations and ratios L_i/L (a_i/H) are; (0.15 (0.2), 0.35 (0.4), 0.55 (0.6)), (0.15 (0.2), 0.35 (0.6), 0.55 (0.4)), (0.15 (0.6), 0.35 (0.4), 0.55 (0.2)), respectively, as indicated $V = 0.5$.

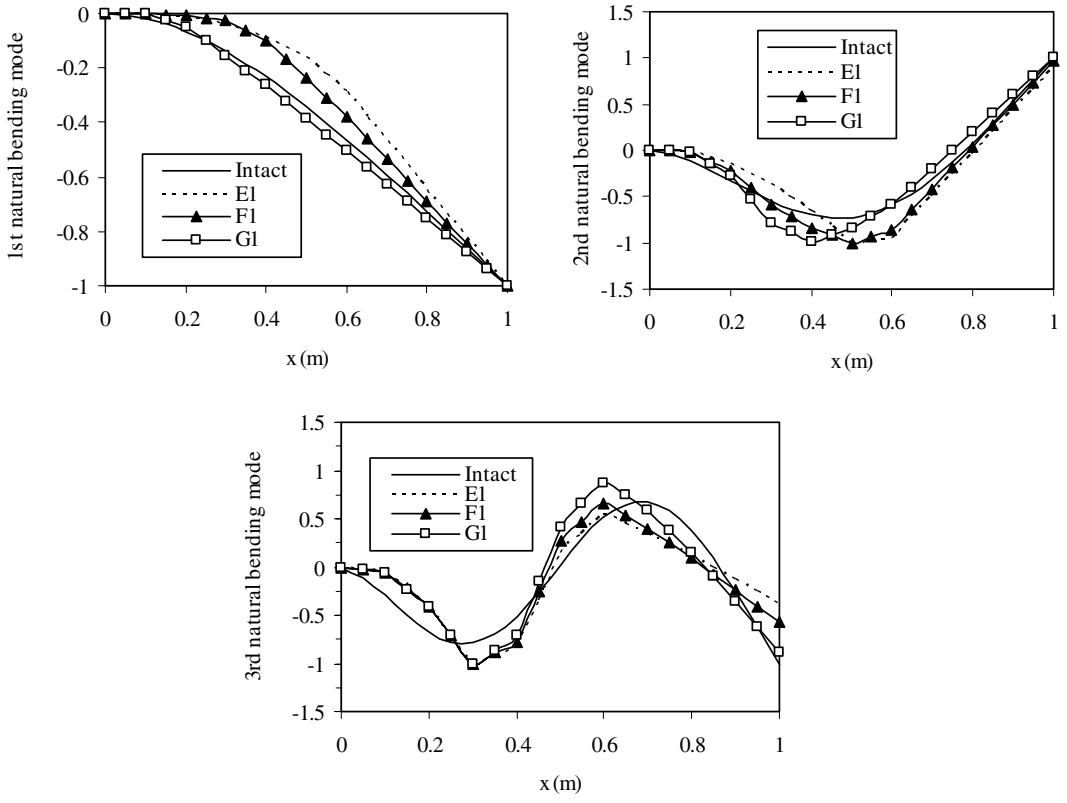

Fig. 12. Normalised first three mode shapes that correspond to the cases in Fig. 11, angle of the fibre α is 0°.

explained as the flexibility due to crack is negligible when the angle of the fibre is greater then 45° [16], especially when the crack ratio is relatively low.

Fig. 10 presents the first three natural frequencies as a function of the volume of the fibre (V) for the several values of the crack ratios (a/H). As the previous case, the composite beam has four cracks which were located as $L_1/L = 0.05$, $L_2/L = 0.35$, $L_3/L = 0.65$, $L_4/L = 0.95$ and the angle of the fibre (α) was 0°. As can be seen from the figure, the natural frequencies are affected by the values of the volume of the fibre (V) and the crack ratios (a/H), as expected. The flexibility due to cracks is high when the volume of the fibre is between 0.2 and 0.8, and maximum when $V = 0.45$ [16]. Therefore, if the volume of the fibre is between 0.2 and 0.8 and the crack ratio is getting higher, the frequency reductions are relatively high, Fig. 10.

In all previous cases, a unique crack depth was considered for the all cracks. Figs. 11 and 12 show the effect of the different crack ratios and the values of the angle of the fibre on the natural frequencies and mode shapes of a composite beam having three cracks. In the analysis three cases, shown as E_1, F_1 and G_1, were considered. The crack locations and ratios (L_1/L (a_1/H), L_2/L (a_2/H), L_3/L (a_3/H)) for the cases E_1, F_1 and G_1, were chosen as, (0.15 (0.2), 0.35 (0.4), 0.55 (0.6)), (0.15 (0.2), 0.35 (0.6), 0.55 (0.4)), (0.15 (0.6), 0.35 (0.4), 0.55 (0.2)), respectively. In the natural frequency analysis, the volume of the fibre (V) was assumed to be 0.5 while in the natural mode shape calculations the volume (V) and angle (α) of the fibre were 0.5 and 0°, respectively. From these figures, it is apparent that the maximum fundamental frequency drop occurs when the large cracks are located closer to the fixed end, while the second and third natural frequencies and mode shapes exhibit higher changes when the large cracks are situated closer to the middle of the beam and at a distance equal to 33% of the beam length from the fixed end, respectively.

5. Concluding remarks

This paper has presented a new method for the numerical modelling of the free vibration of a cantilever composite beam having multiple open and non-propagating cracks. The method integrates the fracture mechanics and the joint interface mechanics to couple substructures. In the methods observed in the literature compromises have been made either in the representation of the physics of the nonlinearities in defective structures or in the complexity of the structure which can be analysed. For example, finite element studies usually use a simplistic representation of the interface mechanics whereas analytical studies require simple boundary conditions. Neither is satisfactory in practical design studies. It is believed that the current approach addresses both of these issues leading to the development of design tools. Consequently, the present approach can be used for the analysis of non-linear interface effects such as contact that occurs when the cracks close. To illustrate the effectiveness of the approach, results have been compared with previous studies published in the literature leading to confidence in the validity of this approach.

Appendix A

The roots of following characteristic equation give the complex constants s_1 and s_2 [24]:

$$\bar{b}_{11}s^4 - 2\bar{b}_{16}s^3 + (2\bar{b}_{12} + \bar{b}_{66})s^2 - 2\bar{b}_{26}s + \bar{b}_{22} = 0,$$

where $\bar{b}_{ij}$ constants are

$$\bar{b}_{11} = b_{11}m^4 + (2b_{12} + b_{66})m^2n^2 + b_{22}n^4,$$

$$\bar{b}_{22} = b_{11}n^4 + (2b_{12} + b_{66})m^2n^2 + b_{22}m^4,$$

$$\bar{b}_{12} = (b_{11} + b_{22} - b_{66})m^2n^2 + b_{12}(m^4 + n^4),$$

$$\bar{b}_{16} = (-2b_{11} + 2b_{12} + b_{66})m^3n + (2b_{22} - 2b_{12} - b_{66})mn^3,$$

$$\bar{b}_{26} = (-2b_{11} + 2b_{12} + b_{66})n^3m + (b_{22} - 2b_{12} - b_{66})nm^3,$$

$$\bar{b}_{66} = 2(2b_{11} - 4b_{12} + 2b_{22} - b_{66})m^2n^2 + b_{66}(m^4 + n^4),$$

where $m = \cos\alpha$, $n = \sin\alpha$ and b_{ij} are compliance constants of the composite along the principal axes. b_{ij} can be related to the mechanical constants of the material by

$$b_{11} = \frac{1}{E_{11}}\left(1 - v_{12}^2\frac{E_{22}}{E_{11}}\right), \quad b_{22} = \frac{1}{E_{22}}(1 - v_{23}^2),$$

$$b_{12} = \frac{-v_{12}}{E_{11}}(1 + v_{23}), \quad b_{66} = 1/G_{12}, \quad b_{44} = 1/G_{23},$$

$$b_{55} = b_{66},$$

where E_{11}, E_{22}, G_{12}, G_{23}, v_{12}, v_{23} and ρ are the mechanical properties of the composite and calculated using the following formulae [24]:

$$\rho = \rho_f V + \rho_m(1 - V), \quad E_{11} = E_f V + E_m(1 - V),$$

$$E_{22} = E_m\left[\frac{E_f + E_m + (E_f - E_m)V}{E_f + E_m - (E_f - E_m)V}\right],$$

$$v_{12} = v_f V + v_m(1 - V),$$

$$v_{23} = v_f V + v_m(1 - V)\left[\frac{1 + v_m - v_{12}E_m/E_{11}}{1 - v_m^2 + v_m v_{12}E_m/E_{11}}\right],$$

$$G_{12} = G_m\left[\frac{G_f + G_m + (G_f - G_m)V}{G_f + G_m - (G_f - G_m)V}\right], \quad G_{23} = \frac{E_{22}}{2(1 + v_{23})},$$

where indices m and f denote matrix and fibre, respectively. E, G, v and ρ are the modulus of elasticity, the

modulus of rigidity, the Poisson's ratio and the mass density, respectively.

References

[1] Cawley P, Adams RD. The location of defects in structures from measurements of natural frequencies. J Strain Anal 1979;14:49–57.

[2] Gouranis G, Dimarogonas AD. A finite element of a cracked prismatic beam for structural analysis. Comput Struct 1988;28:309–13.

[3] Shen MHH, Chu YC. Vibrations of beams with a fatigue crack. Comput Struct 1992;45:79–93.

[4] Ruotolo R, Surace C, Crespo P, Storer D. Harmonic analysis of the vibrations of a cantilevered beam with a closing crack. Comput Struct 1996;61:1057–74.

[5] Kisa M, Brandon JA, Topcu M. Free vibration analysis of cracked beams by a combination of finite elements and component mode synthesis methods. Comput Struct 1998;67(4):215–23.

[6] Kisa M, Brandon JA. The effects of closure of cracks on the dynamics of a cracked cantilever beam. J Sound Vib 2000;238(1):1–18.

[7] Kisa M, Brandon JA. Free vibration analysis of multiple open-edge cracked beams by component mode synthesis. Struct Eng Mech 2000;10(1):81–92.

[8] Wauer J. Dynamics of cracked rotors: a literature survey. Appl Mech Rev 1991;17:1–7.

[9] Dimarogonas AD. Vibration of cracked structures: a state of the art review. Eng Fract Mech 1996;55(5):831–57.

[10] Adams RD, Cawley P, Pye CJ, Stone J. A vibration testing for non-destructively assessing the integrity of the structures. J Mech Eng Sci 1978;20:93–100.

[11] Nikpour K, Dimarogonas AD. Local compliance of composite cracked bodies. Compos Sci Technol 1988;32:209–23.

[12] Nikpour K. Buckling of cracked composite columns. Int J Solids Struct 1990;26(12):1371–86.

[13] Oral S. A shear flexible finite element for non-uniform laminated composite beams. Comput Struct 1991;38(3):353–60.

[14] Krawczuk M. A new finite element for the static and dynamic analysis of cracked composite beams. Comput Struct 1994;52(3):551–61.

[15] Krawczuk M, Ostachowicz WM. Modelling and vibration analysis of a cantilever composite beam with a transverse open crack. J Sound Vib 1995;183(1):69–89.

[16] Krawczuk M, Ostachowicz W, Zak A. Modal analysis of cracked unidirectional composite beam. Compos Part B 1997;28:641–50.

[17] Ruotolo R, Surace C. Damage assessment of multiple cracked beams: numerical results and experimental validation. J Sound Vib 1997;206(4):567–88.

[18] Sekhar AS. Vibration characteristics of a cracked rotor with two open cracks. J Sound Vib 1998;223(4):497–512.

[19] Shifrin EI, Ruotolo R. Natural frequencies of a beam with an arbitrary number of cracks. J Sound Vib 1999;232(3):409–23.

[20] Zheng DY, Fan SC. Natural frequencies of a non-uniform beam with multiple cracks via modified Fourier series. J Sound Vib 2001;242(4):701–17.

[21] Shen MH, Pierre C. Natural modes of Bernoulli–Euler beams with symmetric cracks. J Sound Vib 1990;138(1):115–34.

[22] Song O, Ha TW, Librescu L. Dynamics of anisotropic composite cantilevers weakened by multiple transverse open cracks. Eng Fract Mech 2003;70:105–23.

[23] Hurty WC. Dynamic analysis of structures using substructure modes. AIAA J 1965;3:678–85.

[24] Vinson JR, Sierakowski RL. Behaviour of structures composed of composite materials. 1st ed. Dordrecht: Martinus Nijhoff; 1991.

[25] Tada H, Paris PC, Irwin GR. The stress analysis of cracks handbook. 2nd ed. St. Louis, MO: Paris production incorporated and Del Research Corporation; 1985.

[26] Bao G, Ho S, Suo Z, Fan B. The role of material orthotropy in fracture specimens for composites. Int J Solids Struct 1992;29:1105–16.

[27] Przemieniecki JS. Theory of matrix structural analysis. 1st ed. London: McGraw-Hill; 1967.